Direct Intracranial Injection of AAVrh8 Encoding Monkey β-N-Acetylhexosaminidase Causes Neurotoxicity in the Primate Brain

Diane Golebiowski,[1,2] Imramsjah M.J. van der Bom,[3,4] Churl-Su Kwon,[5] Andrew D. Miller,[6,†] Keiko Petrosky,[6] Allison M. Bradbury,[7,8] Stacy Maitland,[1,2] Anna Luisa Kühn,[3,4] Nina Bishop,[9] Elizabeth Curran,[6] Nilsa Silva,[6] Dwijit GuhaSarkar,[1,2] Susan V. Westmoreland,[6] Douglas R. Martin,[7,8] Matthew J. Gounis,[3,4] Wael F. Asaad,[10,11,12] and Miguel Sena-Esteves[1,2,*]

[1]Department of Neurology, [2]Horae Gene Therapy Center, [3]Department of Radiology, [4]New England Center for Stroke Research, and [9]Department of Animal Medicine, University of Massachusetts Medical School, Worcester, Massachusetts; [5]Department of Neurosurgery, Massachusetts General Hospital, Boston, Massachusetts; [6]New England Primate Research Center, Harvard Medical School, Southborough, Massachusetts; [7]Scott-Ritchey Research Center, [8]Department of Anatomy, Physiology, and Pharmacology, College of Veterinary Medicine, Auburn University, Alabama; [10]Department of Neurosurgery, Alpert Medical School and [11]Brown Institute for Brain Science, Brown University, Providence, Rhode Island; [12]Rhode Island Hospital, Providence, Rhode Island.
[†]Present address: Department of Biomedical Sciences, Section of Anatomic Pathology, Cornell University College of Veterinary Medicine, Ithaca, New York.

GM2 gangliosidoses, including Tay–Sachs disease and Sandhoff disease, are lysosomal storage disorders caused by deficiencies in β-N-acetylhexosaminidase (Hex). Patients are afflicted primarily with progressive central nervous system (CNS) dysfunction. Studies in mice, cats, and sheep have indicated safety and widespread distribution of Hex in the CNS after intracranial vector infusion of AAVrh8 vectors encoding species-specific Hex α- or β-subunits at a 1:1 ratio. Here, a safety study was conducted in cynomolgus macaques (cm), modeling previous animal studies, with bilateral infusion in the thalamus as well as in left lateral ventricle of AAVrh8 vectors encoding cm Hex α- and β-subunits. Three doses (3.2×10^{12} vg [$n=3$]; 3.2×10^{11} vg [$n=2$]; or 1.1×10^{11} vg [$n=2$]) were tested, with controls infused with vehicle ($n=1$) or transgene empty AAVrh8 vector at the highest dose ($n=2$). Most monkeys receiving AAVrh8-cmHexα/β developed dyskinesias, ataxia, and loss of dexterity, with higher dose animals eventually becoming apathetic. Time to onset of symptoms was dose dependent, with the highest-dose cohort producing symptoms within a month of infusion. One monkey in the lowest-dose cohort was behaviorally asymptomatic but had magnetic resonance imaging abnormalities in the thalami. Histopathology was similar in all monkeys injected with AAVrh8-cmHexα/β, showing severe white and gray matter necrosis along the injection track, reactive vasculature, and the presence of neurons with granular eosinophilic material. Lesions were minimal to absent in both control cohorts. Despite cellular loss, a dramatic increase in Hex activity was measured in the thalamus, and none of the animals presented with antibody titers against Hex. The high overexpression of Hex protein is likely to blame for this negative outcome, and this study demonstrates the variations in safety profiles of AAVrh8-Hexα/β intracranial injection among different species, despite encoding for self-proteins.

Keywords: Tay-Sachs disease, hexosaminidase, intracranial delivery, adeno-associated virus, gene therapy, AAV

INTRODUCTION

TAY–SACHS DISEASE (TSD) and Sandhoff disease (SD) belong to a family of lysosomal storage disorders (LSDs) known as GM2 gangliosidoses. Both TSD and SD result from a deficiency in the lysosomal enzyme β-N-acetylhexosaminidase (Hex, hexosaminidase), which breaks down the cellular metabolite GM2 ganglioside into GM3 ganglioside by hydrolyzing the terminal N-acetyl galactosamine residue in the lysosome. HexA is a heterodimer of α- and β-subunits, which are encoded by the *HEXA* and *HEXB* genes, respectively. TSD

*Correspondence: Dr. Miguel Sena-Esteves, Gene Therapy Center, University of Massachusetts Medical School, 368 Plantation Street, ASC6-2055, Worcester, MA 01605. E-mail: miguel.esteves@umassmed.edu

DOI: 10.1089/hum.2016.109

results from mutations in *HEXA*, while SD results from mutations in *HEXB*. Other isozymes of Hex include HexB, a β/β dimer, and HexS, an α/α dimer, neither of which can cleave GM2 ganglioside in humans. HexA deficiency leads to accumulation of GM2 ganglioside in the lysosome, causing dysfunction and eventual cell death. GM2 gangliosidoses primarily affect the central nervous system (CNS), leading to progressive neuronal degeneration.[1]

The three clinical forms of GM2 gangliosidoses are infantile, juvenile, and late-onset. The most severe infantile form is characterized by premature death within the first 5 years of life. Infants develop normally for the first 6 months, and patients are usually diagnosed at approximately 1 year of age due to regression of or failure to reach developmental milestones. Symptoms include seizures, deficits in motor functions, and dysphagia. Patients eventually decline to a vegetative state before succumbing to the disease. Presently, the care for these patients consists of palliative measures because there is no effective treatment.[2]

The current treatment for many LSDs is enzyme replacement therapy (ERT), where recombinant enzyme is delivered repeatedly, usually through intravenous or intramuscular injections.[3] However, due to the inability of lysosomal enzymes to cross the blood–brain barrier (BBB), this strategy is ineffective to treat the majority of LSDs, which have a CNS component, including TSD and SD.[4,5]

Gene therapy has proven to be one of the most promising approaches for treating many LSDs, with the potential to be a permanent, one-time treatment that can circumvent the issues associated with the BBB and recombinant enzyme delivery. Both ERT and gene therapy utilize the cross-correction mechanism where lysosomal enzymes secreted by a cell, especially when overexpressed, can be taken up by neighboring cells through the mannose-6-phosphate receptor and targeted correctly to the lysosome. Therefore, stable gene delivery to a relatively small subset of cells may be sufficient to supply the entire body with therapeutic levels of the missing enzyme. In the brain, distribution of lysosomal enzymes occurs through diffusion,[6] cerebral spinal fluid (CSF) flow,[7–9] and axonal transport.[10–15]

Recombinant adeno-associated virus (AAV) vectors have become the leading platform for development of *in vivo* gene therapies for LSDs with neurological involvement, as they transduce dividing and non-dividing cells in the CNS at high efficiency, and mediate long-term gene expression with minimal or no toxicity.[16] The most effective gene therapy approaches based on intracranial infusion of AAV vectors have targeted structures highly interconnected with other regions of the brain such as the striatum,[17–19] ventral tegmental area,[20] deep cerebellar nuclei (DCN),[21] thalamus,[22] or CSF.[8,23,24] These intracranial delivery strategies reduce the number of injections necessary to achieve widespread distribution of lysosomal enzymes in the brain and have demonstrated efficacy in large animal models of different LSDs.[25–32]

SD mice and cats, and TSD sheep are the three available animal models of GM2 gangliosidoses whose phenotypes mimic the symptoms seen in human patients. Traditionally, both *HEXA* and *HEXB* genes are delivered to both SD and TSD animal models in order to produce ideal HexA isozyme overexpression.[33–35] SD mice ($Hexb^{-/-}$) were generated by targeted disruption of *Hexb*. SD mice have been treated by intracranial injections of a combination of two AAV vectors, encoding human Hex α- and Hex β-subunits. Treated SD mice live as long as 2 years, or the normal life-span of wild-type mice.[17,25,26] Both the SD cat and TSD sheep are naturally occurring large animal models that accumulate GM2 ganglioside and show neurological and motor dysfunction as well as a reduction in life-span, living approximately 4.5 and 9 months, respectively.[25,36,37] SD cats have a 25-base pair inversion in the 3′ end of *Hexb* that results in <3% residual enzyme activity in brain.[38] TSD sheep carry a mutation in the *Hexa* gene that leads to skipping of exon 11, and thus HexA activity to the artificial substrate 4-methylumbelliferyl 6-sulfo-2-acetamido-2-deoxy-β-D-glucopyranoside potassium salt (MUGS) is reduced to 6% and 29% of normal in liver and brain, respectively.[36] Simultaneous delivery of two AAVrh8 vectors encoding feline Hex α- and Hex β-subunits has been successful in treating feline SD CNS pathology and extending life-span through bilateral injection into the thalamus alone or in combination with the DCN.[25,26] Unpublished data from the authors' lab has demonstrated similar efficacy in treating SD mice using AAVrh8 vectors encoding mouse Hex subunits, as shown previously for other AAV constructs.[17,39] Furthermore, a single injection of AAV vectors into the cerebral lateral ventricle (ICV) is as effective as DCN injection in complementing the therapeutic effect of bilateral thalamic injections in mice and cats.[27] Because ICV injection is considered safer than DCN injection, preclinical safety studies were conducted using bilateral thalamic injections in combination with ICV delivery of an equimolar formulation of two AAVrh8 vectors encoding Hex α- and Hex β-subunits.[16]

Many preclinical safety studies have been conducted in nonhuman primates (NHPs) due to phy-

logenetic similarities, allowing testing of the feasibility of scale-up from rodent models to humans. Numerous studies have been conducted in NHPs to assess safety of AAV gene therapy for metabolic and neurological diseases using systemic, cerebrospinal fluid, and intracranial delivery routes.[40–47] However, such safety studies differ widely in delivery route, AAV vector design/dosing, therapeutic gene, and volume/rate of injection. Thus, extrapolation of safety to this paradigm is not advisable, as a novel capsid (AAVrh8) and target (thalamus) is being used, which have never been tested in humans. Previous studies using direct intracranial injections of AAVrh8 vectors encoding species-specific Hex α- or β-subunits at 1:1 ratio in mice, cats, and sheep have all indicated safety, widespread enzyme distribution, and therapeutic efficacy.[25,27] In the present study, the gene therapy strategy used in SD cats was tested for preclinical safety and feasibility using normal monkeys.

MATERIALS AND METHODS

AAVrh8-CBA-Hexα/β-WPRE $^{mut6\Delta ATG}$ vector production

A single-stranded rAAV vector plasmid described previously[48] was used to generate the AAVrh8-CBA-cmHexα-WPRE$^{mut6\Delta ATG}$ and AAVrh8-CBA-cmHexβ-WPRE$^{mut6\Delta ATG}$ plasmids. The woodchuck hepatitis virus post-transcriptional regulatory element was modified to include the previously described mut6 mutations in the putative promoter region of protein X,[49] as well as replace all putative ATG codons with TTG. This modified WPRE$^{mut6\Delta ATG}$ was synthesized by overlapping polymerase chain reaction (PCR). Modified WPRE sequence: GATAATCAA CCTCTGGATTACAAAATTTGTGAAAGATTGAC TGGTATTCTTAACTTTGTTGCTCCTTTTACGC TTTGTGGATACGCTGCTTTATTGCCTTTGTAT CTTGCTATTGCTTCCCGTTTGGCTTTCATTTT CTCCTCCTTGTATAAATCCTGGTTGCTGTCTC TTTTTGAGGAGTTGTGGCCCGTTGTCAGGCA ACGTGGCGTGGTGTGCACTGTGTTTGCTGAC GCAACCCCCACTGGTTGGGGCATTGCCACCA CCTGTCAGCTCCTTTCCGGGACTTTCGCTTTC CCCCTCCCTATTGCCACGGCGGAACTCATCG CCGCCTGCCTTGCCCGCTGCTGGACAGGGGC TCGGCTGTTGGGCACTGACAATTCCGTGGTG TTGTCGGGGAAATCATCGTCCTTTCCTTGGC TGCTCGCCTGTGTTGCCACCTGGATTCTGCG CGGGACGTCCTTCTGCTACGTCCCTTCGGCC CTCAATCCAGCGGACCTTCCTTCCCGCGGCC TGCTGCCGGCTCTGCGGCCTCTTCCGCGTCT TCGCCTTCGCCCTCAGACGAGTCGGATCTCCC TTTGGGCCGCCTCCCCGCATCGGACTAG.

AAVrh8 vectors were produced by triple transient transfection of 293T cells followed by purification using iodixanol gradient and fast protein liquid chromatography, as previously described.[50] Vectors were then concentrated using Acrodisc® Units with Mustang® Q Membranes (Pall Corporation), buffer exchanged to phosphate-buffered saline (PBS) using 10 kDa Slide-A-Lyzer™ Dialysis Cassettes (Thermo Fisher Scientific), and filtered using Millex-GV Syringe Filter Unit, 0.22 μm, PVDF, 4 mm (EMD Millipore). The titers of the vectors were measured by real-time quantitative PCR with primers and probe to the bovine growth hormone polyadenylation signal, as described previously.[50]

ANIMALS

Male and female cynomolgus macaques (cm; 1.5–2.5 years old) were purchased from Worldwide Primates, Inc. and selected for this study based on the absence of AAVrh8 neutralizing antibodies in serum (<1:10), measured as previously described.[51] All experiments were reviewed and approved by the Institutional Animal Care and Use Committee at the University of Massachusetts Medical School, and performed in compliance with the National Institutes of Health Guide for Care and Use of Laboratory Animals, 8th edition.

INTRACEREBRAL INJECTION OF AAVRH8 VECTORS OR PBS AND IMAGING IN ANIMALS

Three doses (3.2×10^{12} vg [$1\times$cohort, $n=3$], 3.2×10^{11} vg [1/10th cohort, $n=2$], or 1.1×10^{11} vg [1/30th cohort, $n=2$]) containing a 1:1 ratio of AAVrh8 vectors encoding cmHexα- and cmHexβ-subunits, along with control groups injected with vehicle (PBS, $n=1$) or 3.2×10^{12} vg of an AAVrh8 vector without a transgene (TGE, $n=2$), were tested. Neurosurgical procedure, injection, and imaging were performed as previously described.[16,52,53] Targeting and trajectory planning occurred through fusion of live operative fluoroscopy and cone-beam computed tomography scans with presurgical magnetic resonance imaging (MRI). Bilateral injections into the thalamus occurred simultaneously (150 μL per side) with an infusion rate of 2 μL/min using a 16G SmartFlow™ neuroventricular cannula (MRI Interventions, Inc.). Approximately 10 min after infusion, the cannulas were withdrawn from the brain and followed by injection into the left cerebral lateral ventricle (300 μL) at a rate of 50 μL/min using a 16G SmartFlow™ neuroventricular cannula (MRI Interventions, Inc.). In all cohorts, each thalamus received 1/4th of the total AAV vector dose, and the left cerebral lateral

ventricle received half. Injection volumes were kept constant across cohorts.

Clinical monitoring and neurological assessment

Monkeys were assessed in their home cage before surgery and weekly as described.[54] Behavior of monkeys in their home cage was also evaluated using a camcorder to document behavior before surgery and at 7, 15, 30, 60, and 90 days post surgery. Spontaneous behavior (recording the monkey for 3.5 min while absent from the room), food presentation and response (to handing animal treats or placing treats in the food hopper for 1 min), and response to threat (approaching animal's cage while looking directly at the monkey for 1 min) were all documented.

Measurement of antibody titers in serum

Serum antibody titers toward AAVrh8 vector or purified human Hex α-subunit (Sigma–Aldrich) were measured using an enzyme-linked immunosorbent assay (ELISA), as previously described.[25] Titers ≤1:8 were considered not detectable.

Tissue collection, processing, histopathology, histochemistry, and immunohistochemistry

Fresh, unperfused tissue was collected from animals in the highest-dose cohort (3.2×10^{12} vg) as well from the PBS control group. Animals from the 3.2×10^{11} vg dose cohort, 1.1×10^{11} vg dose cohort, and control animals receiving AAVrh8 vector without a transgene were perfused with cold PBS prior to tissue collection. Following death, a complete necropsy was performed. All tissues collected were fixed in 10% neutral buffered formalin and were paraffin embedded according to standard procedures. Five micrometers of histologic sections were routinely processed and stained with hematoxylin and eosin (H&E). Luxol fast blue histochemical staining was performed based on standard procedures. To characterize the immune cell infiltrate of the lesions, immunohistochemistry for CD3, CD20, and CD68 was performed. Briefly, all staining protocols used an antigen retrieval protocol of microwaving in 0.1 M of sodium citrate buffer for 20 min followed by 20 min of cooling at room temperature (RT). CD3 (Dako; catalog #A0452) was applied for 30 min at room temperature at a dilution of 1:600. CD20 (Dako; catalog #M0755) and CD68 (Dako; catalog #M0814) were applied overnight at 4°C at a dilution of 1:179 and 1:410, respectively. Secondary antibodies were biotinylated horse anti-mouse (Vector Laboratories) or biotinylated goat anti-rabbit (Vector Laboratories) as appropriate, diluted 1:200, and incubated for 30 min at room temperature. Tertiary reagent in each case was Vectastain ABC Elite reagent (CD3) or Vectastain ABC Standard reagent (CD20, CD68) incubated for 30 min at RT (Vector Laboratories). All slides were developed with DAB chromogen (Dako) and counterstained with Mayer's hematoxylin. Negative controls consisted of identical brain sections stained with irrelevant species-, isotype-, and concentration-matched antibodies. A lymph node served as the control tissue for all antibodies.

Western blotting

Tissues were lysed from 3 mm of biopsy punches of the thalamus in T-PER™ Tissue Protein Extraction Reagent (Thermo Scientific) containing cOmplete Protease Inhibitor Cocktail (Roche). Total protein was measured using QuickStart™ Bradford Protein Assay with serial dilutions of bovine serum albumin as protein standard (Bio-Rad). Total protein lysates (20 μg) were resolved using SDS-polyacrylamide gel electrophoresis with 4–20% Mini-PROTEAN® TGX™ (Bio-Rad) precast gel in 25 mM Tris 190 mM Glycine 0.1% sodium dodecyl sulfate followed by wet transfer to a 0.22 μm nitrocellulose membrane (Maine Manufacturing, LLC) in 25 mM Tris 190 mM Glycine. Membranes were blocked for 1 h in 5% nonfat dry milk in Tris-buffered saline with 0.05% Tween™ 20 (TBST) and probed with rabbit anti-Hex α-subunit antibody (LifeSpan BioSciences, Inc.) or mouse anti-Hex β-subunit antibody[25] diluted 1:1,000 in 5% nonfat dry milk in TBST and incubated overnight at 4°C. Horseradish peroxidase (HRP)-conjugated secondary antibodies (anti-mouse or anti-rabbit; GE Healthcare) were diluted 1:5,000 in 5% nonfat dry milk TBST and incubated for 1 h at room temperature. Signal was detected using Pierce ECL Western Blotting Substrate (Thermo Fisher Scientific) followed by exposure to Amersham Hyperfilm ECL (GE Healthcare). Membranes were stripped using 100 mM glycine (pH 4.0) for 25 min, washed in TBST, and then blocked and probed again using HRP-conjugated mouse anti-β-actin antibody (GenScript) diluted 1:1,000 in 5% nonfat dry milk in TBST for 1 h and detected as before.

Hexosaminidase activity

Hexosaminidase isozyme activities were measured from fresh frozen tissue either from 3 mm biopsy punches from the thalamus of 4 mm coronal blocks or from 2 mm slices from thoracic spinal cord coronal blocks using 4-methylumbelliferyl N-acetyl-β-D-glucosaminide (MUG; Sigma) and MUGS (Toronto Research Chemicals), and normalized to total protein measured by QuickStart™ Bradford Protein

Assay with serial dilutions of bovine serum albumin as protein standard (Bio-Rad), as previously described.[25] Enzyme activity is represented as nmol 4MU/h/mg protein.

Fluorescent immunostaining

Formalin-fixed paraffin sections (5 μm thick) were used for neuropathological evaluation. Paraffin was removed from tissue-mounted slides with two 8 min incubations in xylenes and then rehydrated with serial 4 min incubations in 100%, 95%, and 80% ethanol followed by 1× PBS. For antigen retrieval, slides were boiled in 10 mM Tris 1 mM EDTA (pH 9.0) for 5 min and then cooled for 20 min. Blocking with permeabilization was done for 1 h in 5% normal goat serum (SouthernBiotech) in PBS with 0.05% Tween-20 (Acros). Sections were incubated with primary antibodies diluted in 5% normal goat serum in PBS with 0.05% Tween-20 for 1 h at room temperature at the following concentrations: rabbit anti-HEXA, 1:1,000 (LifeSpan BioSciences, Inc.), mouse anti-HEXB, 1:1,000,[25] or NeuN, 1:1,000 (EMD Millipore). Sections were washed three times in TBST, and secondary antibodies against the appropriate species and conjugated to the different fluorophores (Alexa-488 or Alexa-555; Thermo Fisher Scientific) were diluted 1:1,000 in 5% normal goat serum in PBS with 0.05% Tween-20 and incubated for 30 min followed by three washes in PBS. Sections were stained for 1 min in Thermo Fisher Scientific Pierce™ DAPI Nuclear Counterstain diluted in PBS. Coverslips were mounted on slides using PermaFluor aqueous mounting medium (Thermo Fisher Scientific).

In situ hybridization

RNAscope fluorescent multiplex kit (Advanced Cell Diagnostics) was used for *in situ* analysis of vector derived mRNA in tissue sections using a $WPRE^{mut6\Delta ATG}$ specific probe set (Advanced Cell Diagnostics). Formalin-fixed 4 μm paraffin brain sections were used according to the manufacturer's instructions.

Silver stain of AAVrh8 vector and densitometry

AAVrh8 vector purity was assessed by gel electrophoresis using 4–20% Mini-PROTEAN® TGX™ (Bio-Rad) precast gels followed by silver staining (Invitrogen) and densitometry.

Electron microscopy of AAVrh8 vector preparations

AAVrh8 vector preparations were analyzed by the Core Electron Microscopy Facility at the University of Massachusetts Medical School (Worcester, MA) using negative staining.

Endotoxin detection

Endotoxin levels were measured on AAV vector preparations using the Endpoint Chromogenic LAL Assays (QCL-1000™) from Lonza, according to the manufacturer's instructions.

RESULTS

Experimental design

The goal of this study was to assess the safety of a formulation of two AAVrh8 vectors (1:1 ratio) encoding Hex α- and β-subunits injected bilaterally into the thalamus and one cerebral lateral ventricle in cm (Supplementary Fig. S1; Supplementary Data are available online at www.liebertpub.com/hum). Vector purity, endotoxin levels, and empty capsid ratios were measured (Supplementary Fig. S1). These vectors encoded cm Hex proteins to reduce the likelihood of a confounding immune response triggered by delivery of Hex proteins from other species. All subjects were selected for the absence of AAVrh8 neutralizing antibody titers (<1:10). The study included three dosing cohorts: 3.2×10^{12} vg (1×cohort, $n=3$), 3.2×10^{11} vg (1/10th cohort, $n=2$), and 1.1×10^{11} vg (1/30th cohort, $n=2$) of AAVrh8-cmHex vectors. Control groups were injected with vehicle (PBS, $n=1$) or 3.2×10^{12} vg of a TGE AAVrh8 vector ($n=2$). The 1×dose was based on the efficacious dose in SD cats by vg/kg brain weight.[27] Safety was determined by neurological behavioral assessments, MRI data obtained at the study endpoint (90 days), and pathological examination of tissues.

Clinical observations

All monkeys tolerated and recovered well from the surgical procedure. However, monkeys in the highest-dose cohort (1×) started to show neurological symptoms at 2–3 weeks after the injection. Symptoms included general weakness of limbs, ataxia, inability to perch, and reduced food intake. The neurological function of these animals declined rapidly, and they became apathetic, which led to premature euthanasia between 20 and 28 days. In the 1/10th dosing cohort, animals appeared normal until 33 and 48 days after the injection when they began to develop chorea and dyskinesia during voluntary movement, such as when reaching out for food. From this cohort, the animal that developed symptoms at 33 days required euthanasia at 57 days due to lethargy and unresponsiveness. However, the other animal in this cohort survived to the 90-day study endpoint. In the 1/30th dosing cohort, one animal lost voluntary use of its right arm at 59 days and required euthanasia due to

Table 1. *Summary of neurological symptoms observed in study animals*

Animal ID	*Vector dose*	*Symptom onset (days)*	*Survival (days)*	*Clinical signs*
0908068	1×	14	20	Lethargy, unresponsive
0908087	1×	17	23	Ataxia, unable to perch
0909589	1×	27	28	Generalized weakness especially of right leg, reduced food intake
8722431552	1/10th	33	57	Dyskinesias, chorea
09087133	1/10th	48	≥ Endpoint	Dyskinesias, chorea
0909587	1/30th	59	66	Loss of voluntary use of right arm, eventual lethargy
0908997	1/30th	n/a	≥ Endpoint	None
8963934563	PBS	n/a	≥ Endpoint	None
5347096796	TGE (1×)	n/a	≥ Endpoint	None
7667353701	TGE (1×)	n/a	≥ Endpoint	None

For each animal, vector dose, day of symptom onset, length of survival, and observed clinical signs are indicated. The predetermined endpoint of the study was 90 days.
TGE, transgene empty; PBS, phosphate-buffered saline.

lethargy at 66 days. The other animal in this cohort did not develop any major clinical signs and survived to the 90-day study endpoint (Table 1). Despite no outward clinical symptoms in this animal, a brain MRI before necropsy indicated alterations in the thalamus (Fig. 1). No clinical signs were observed in the control cohorts, which consisted of a PBS-injected animal, as well as two animals injected with a TGE AAVrh8 vector at the 1×dose (Table 1 and Fig. 1).

Pathology

Serum antibody titers to human recombinant HexA and AAVrh8 capsid were measured both before the injection and at necropsy. There were no detectable titers to the HexA protein before the injection or at necropsy in all animals. At necropsy, animals receiving vector (including the TGE control) had AAVrh8 capsid serum antibody titers ranging from 1:128 to 1:49,152. The PBS-injected animal did not have any AAVrh8 capsid antibody titers (Table 2).

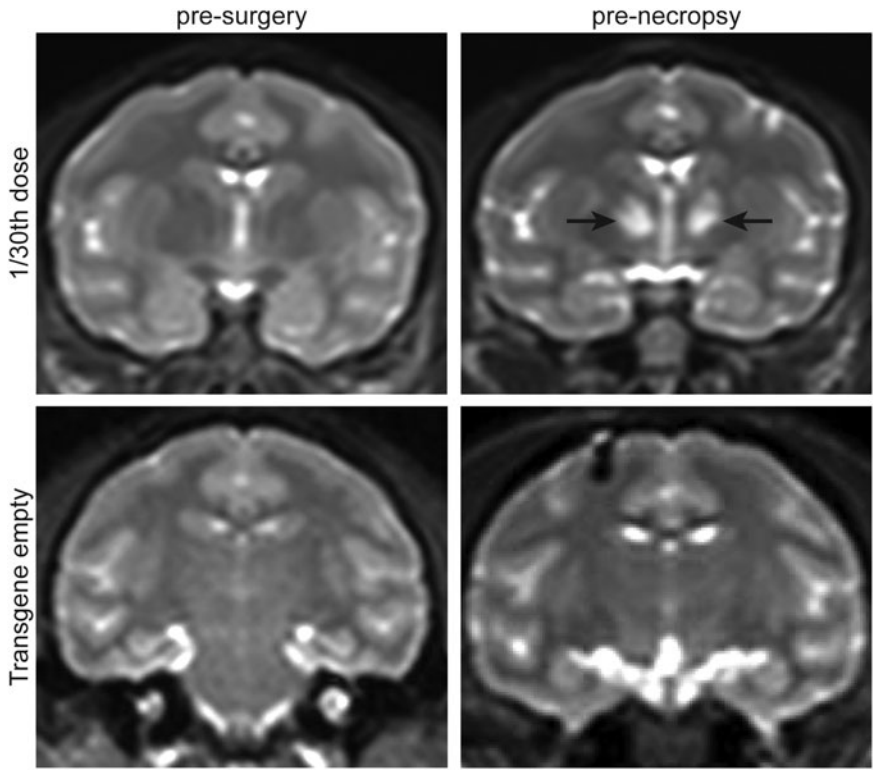

Figure 1. Corresponding coronal sections of brain T2-weighted magnetic resonance imaging before surgery and before necropsy indicating signal alterations at the study endpoint in the treated animal. Hyper-intensities (*arrows*) detected in the thalami of an animal injected with 1.1×10^{11} vg (1/30th dose) of AAVrh8 vector formulation encoding cmHexα or cmHexβ subunits. No hyper-intensities were noted at any time point in the thalami of animals treated with a transgene empty vector.

Table 2. *Serum titers against recombinant human Hexα-subunit and AAVrh8 capsid*

	Titer to hHex α-subunit		*Titer to rh8 capsid*	
Animal ID	*Before surgery*	*At necropsy*	*Before surgery*[a]	*At necropsy*
1×				
0908068	ND 1:8	ND 1:8	ND	1:3,072
0908087	ND 1:8	ND 1:8	ND	1:2,048
0909589	ND 1:8	ND 1:8	ND	1:1,024
1/10th				
8722431552	ND 1:8	ND 1:8	ND	1:49,152
09087133	ND 1:8	ND 1:8	ND	1:49,152
1/30th				
0909587	ND 1:8	ND 1:8	ND	1:128
0908997	ND 1:8	ND 1:8	ND	1:384
PBS				
8963934563	ND 1:8	ND 1:8	ND	ND 1:8
TGE				
5347096796	ND 1:8	ND 1:8	ND	1:49,152
7667353701	ND 1:8	ND 1:8	ND	1:1,024

The titers before surgery and at necropsy measured by enzyme-linked immunosorbent assay against Hexα and AAVrh8 capsid for each animal and their dosing cohorts are indicated.

[a]Presurgery AAVrh8 titers were measured by neutralizing antibody screen to select animals.

ND, not detected.

Histological examination of the brain revealed widespread neuropathology in the thalamus of animals injected with AAVrh8 encoding Hex. Alterations included the presence of granular eosinophilic inclusions in neurons (Fig. 2A), necrotic areas with cellular loss and vacuolation (Fig. 2B), perivascular cuffing (Fig. 2C), and white-matter loss indicated by lack of luxol fast blue stain (Fig. 2D). Neurons with eosinophilic inclusions were also observed in the thalamus of the other NHPs injected with lower doses of AAVrh8-cmHex vectors (Fig. 2E). There was no evidence of neuropathology in other regions of the brain, with the exception of that associated with needle tracks. All control cohorts had mostly normal histological appearance in the thalamus (Fig. 2F), with only small lesions present near the injection site or needle tracks.

Analysis of the types of immune cells by immunohistochemistry revealed the presence of T cells ($CD3^+$) and B cells ($CD20^+$) in perivascular cuffs, but little to none elsewhere in the thalamus (Fig. 3A and B). However, there was a large macrophage/microglial presence, as shown in CD68 immunostaining in the thalamus (Fig. 3C). These findings were common to all subjects treated with AAV-cmHex vectors, but not in NHPs treated with either PBS or TGE AAV vector.

Hexosamindase expression and localization

Western blot analysis of Hex α- and Hex β-subunit protein levels revealed increased levels in the thalamus of animals injected with AAVrh8 vectors encoding cmHexα/β (Fig. 4A). Accordingly, hexosaminidase activity in the thalamus and spinal cord of animals injected with AAVrh8 vectors encoding cmHexα/β was considerably higher than in control animals, in some instances by >100-fold (Fig. 4B). This large increase in hexosaminidase expression was still present, despite the cellular loss observed in the thalamus (Fig. 2).

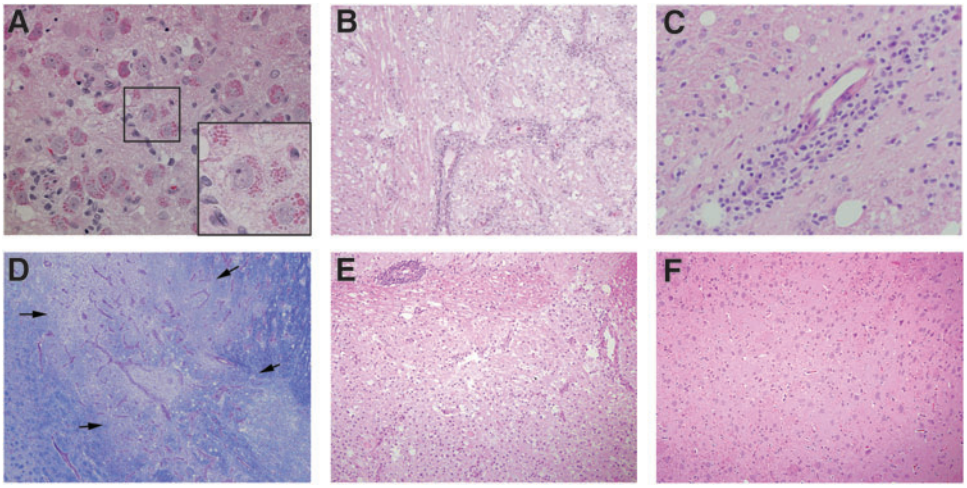

Figure 2. Histological findings in the thalamus. (**A**) Neurons with granular eosinophilic inclusions were present in the thalamus of AAVrh8-Hex injected animals. *Box* indicates location of magnified region. 40×. (**B**) Necrotic area in the thalamus with cell loss and vacuolation. 10×. (**C**) Example of perivascular cuffing in the thalamus. 20×. (**D**) Luxol fast blue staining revealed a large area (delineated by *arrows*) of necrosis, vascular proliferation, and white matter loss (note *pallor* compared to adjacent *dark blue color*). 10×. (**E**) Neuropathological findings were identical in the lowest dosing cohort. 10×. (**F**) Normal histology of the thalamus in phosphate-buffered saline (PBS)-injected animal; 10×(1× cohort, **A**–**D**; 1/30th cohort, **E**; PBS-injected, **F**). Tissue sections for histological assessment shown in (**A**), (**B**), (**C**), (**E**), and (**F**) were stained with hematoxylin and eosin.

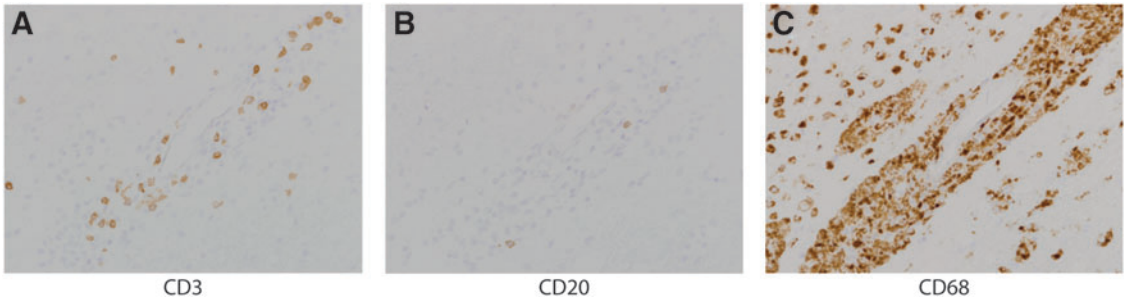

Figure 3. Immunological profile of perivascular cuffs in AAVrh8-cmHexα/β injected monkey thalamus. (**A**) CD3 immunostaining for T cells. (**B**) CD20 immunostaining for B cells. (**C**) CD68 immunostaining for macrophages/microglia. (**A**–**C**; 1/10th cohort animal). 20×.

Despite cellular loss (Fig. 2), there were still numerous cells in the thalamus containing supraphysiological levels of both Hex subunits, as shown by double immunofluorescence staining for Hex α- and Hex β-subunits (Fig. 5A). Many of these cells were neurons given the co-localization of Hex α-subunit with NeuN (Fig. 5B). *In situ* hybridization in parallel sections using a WPRE probe indicated many AAV vector transduced cells (Fig. 5C).

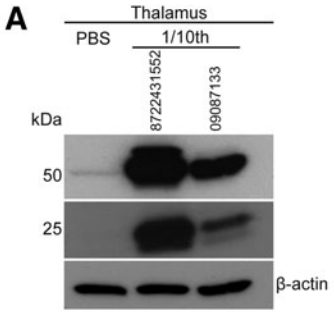

B

Animal ID (dose)		Thalamus 4-MU nmol/hour/mg MUG	Thalamus 4-MU nmol/hour/mg MUGS	Thoracic Spinal Cord 4-MU nmol/hour/mg MUG	Thoracic Spinal Cord 4-MU nmol/hour/mg MUGS
908068 (1x)	left	6782	2231	1491	541
	right	31603	14626		
908087 (1x)	left	10982	3590	2524	765
	right	21704	9000		
909589 (1x)	unknown	42675	19371	1809	596
8722431552 ($1/10^{th}$)	left	70472	26273	1186	359
	right	93951	32650		
9087133 ($1/10^{th}$)	left	14996	5073	1435	352
	right	17151	5722		
909587 ($1/30^{th}$)	left	7836	2465	974	289
	right	5391	1972		
908997 ($1/30^{th}$)	left	26919	11487	940	265
	right	18202	6438		
8963934563 (PBS)	left	919	184	522	182
	right	981	191		
5347096796 (TGE 1x)	left	1847	349	509	212
	right	971	200		
7667353701 (TGE 1x)	left	1121	296	599	174
	right	1236	323		

Figure 4. Increased Hex expression and activity in the central nervous system. (**A**) Western blot analysis of Hex α- or β-subunit protein levels in thalamus lysates from the PBS-injected control and two animals from the 1/10th cohort. (**B**) Hex activity was measured in the thalamus and thoracic spinal cord on all cohorts. 4-Methylumbelliferyl N-acetyl-β-D-glucosaminide substrate is cleaved by HexA, HexB, and HexS isozymes. 4-Methylumbelliferyl 6-sulfo-2-acetamido-2-deoxy-β-D-glucopyranoside potassium salt substrate is preferentially cleaved by HexA and HexS isozymes. Note: Due to an emergency euthanasia and necropsy, the identity of the thalamus (left or right) in animal is 909589 is unknown.

DISCUSSION

Production of Hex through direct thalamic delivery of AAVrh8 vectors encoding species-specific subunits proved to be toxic in normal NHPs, probably due to overexpression. The severe neurological symptoms that manifested over time were surprising, given the demonstrated efficacy and safety of bilateral injections of AAV-Hex vectors (AAV1, AAV2, and AAVrh8) in normal and GM2 affected disease mice, cats, and sheep.[17,25,27,39] The absence of neuropathology elsewhere in the CNS suggests that delivery of AAVrh8-Hex vectors into CSF through the cerebral lateral ventricles is safe.

The most likely explanation for the neurologic deterioration is the extensive cellular loss in the thalamus, revealed by neuropathological examination of the NHP brains injected with AAVrh8-cmHexα/β. Unlike the severe histological findings documented here, a prior study in NHPs injected with an AAV2 vector expressing human acid sphingomyelinase in the thalamus and brain stem also developed severe neurological symptoms but with no apparent cellular loss. Instead, there was robust infiltration of injected brain structures with inflammatory cells.[55]

Several lines of evidence in the present study suggest the degenerative process triggered by thalamic injection of AAVrh8-cmHexα/β vectors in normal NHPs is unlikely to have been caused by an immunological response. The human and cm hexosamindase α- and β-subunits differ by 11 and 23 amino acids, respectively (Supplementary Figs. S2 and S3). Intracranial injection of AAV vectors encoding non-self-proteins in NHPs and other species has been shown to trigger strong immune responses, resulting in extensive cellular loss. In addition to the

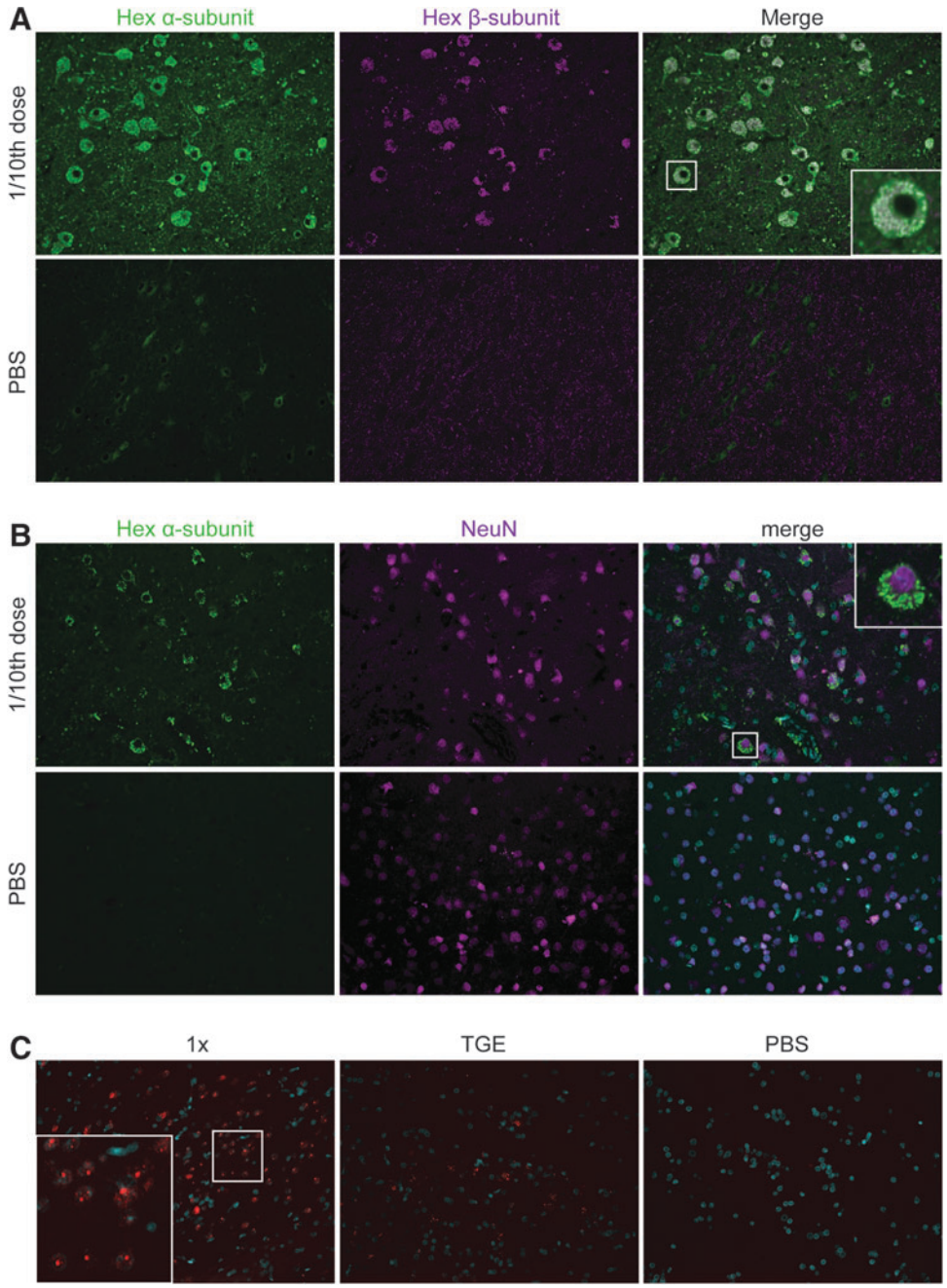

Figure 5. Hexα- or Hexβ-subunit localization in monkey thalamus. (**A**) Immunofluorescence staining for Hexα (*green*) and Hexβ (*magenta*) subunits and their co-localization (*white*). *Box* indicates location of magnified region. 40×. (**B**) Immunostaining for Hexα-subunit (*green*) and NeuN (*magenta*). 40×. (**C**) RNA *in situ* hybridization with probe for WPRE (*red*) expressed by AAV transduced cells. DAPI stain (*cyan*). 20×.

antigenic nature of the transgene, the AAV capsid tropism to antigen presenting cells in the brain may also be a contributing factor.[56,57] Moreover, as patients afflicted with lysosomal storage diseases treated by enzyme replacement therapy often develop antibodies to recombinant human proteins,[58,59] the differences in Hex subunits between species may be a significant factor that could confound the interpretation of the results. As such, the AAVrh8-Hex vectors encoded cm hexosamindase α- and β-subunits, which would make it unlikely that cellular loss was caused by an adaptive immune response to the transgenes. The presence of large numbers of transduced neurons in the thalamus near areas of heavy cellular loss further supports the notion of a non-immune mechanism. In addition, inflammatory cells in the thalamus were mostly of the macrophage lineage ($CD68^+$), with very few $CD3^+$ T cells only found near some blood vessels. These findings suggest that the inflammatory cell

infiltration was likely secondary to a primary neurodegenerative insult. Also, no evidence was found of antibodies to HexA at the endpoint, although this finding has a caveat that the ELISA assay was based on commercially available human Hex, and thus it is possible that it failed to detect antibodies to NHP specific epitopes.

Despite having low or absent neutralizing antibodies to AAVrh8 (titer <1:10) prior to injection, all NHPs injected with AAVrh8 vectors had high anti-capsid antibody titers at the endpoint. However, a humoral response to the capsid is unlikely to have a significant contribution to the cellular loss, as control NHPs injected with the transgene-empty AAVrh8 vector showed no evidence of neuropathology beyond that associated with the needle track. Moreover, previous studies have reported the presence of high anti-AAV antibody titers after intracranial delivery in NHPs with no apparent adverse effects.[46,47]

Despite extensive cellular loss, Hex activity in the thalamus of NHP injected with AAVrh8-cmHexα/β vector was >100-fold above normal. These high Hex expression levels appear to be driven by the remaining transduced neurons laden with eosinophilic granules filled with Hex, as indicated by co-immunofluorescence staining with antibodies to Hex α- and β-subunits. Neurons with identical intracellular features were also found in the thalamus of long-lived cats treated with AAVrh8 vectors encoding feline Hex subunits, but with no evidence of cellular loss or neurological deficits.[25] Transgenic mice overexpressing lysosomal beta-glucuronidase (GUSB) also displayed eosinophilic granules in different cell types, and brain expression levels were $\sim$100–700-fold above normal, with no apparent neurological deficits. This indicates that massive overexpression of at least GUSB in neurons is well tolerated.[60] However, there are fundamental differences between transgenesis and AAV-mediated *de novo* overexpression, namely developmental adaptation of cellular pathways to high-level expression of a lysosomal enzyme. Also, tissue level activity in transgenic mice is likely the result of relatively uniform enzyme activity in most cells in the tissue. On the other hand, the efficiency of AAV gene delivery to the brain by intraparenchymal injection is far from achieving transduction of all cells in a particular structure, and thus the measured activities are the result of enzyme expression in a subset of cells. The >100-fold above normal HexA levels in the thalamus of AAVrh8 injected NHPs at the endpoint appeared to be produced by a relatively small number of neurons, and thus it is likely that activities in those cells are considerably higher than the average measured in tissue punches but are still compatible with survival. It seems reasonable to postulate that HexA expression crossed an unknown threshold in some cells that triggered a neurodegenerative process. A possible mechanism is that continuous high-level expression of HexA overtaxes the protein folding capacity in some AAV transduced neurons, leading to a chronic unfolded protein response that ultimately results in cell death.[61] The exact limit of overexpression tolerated by neurons is unknown, but the notion that lysosomal enzymes can be expressed at any level with no consequences to genetically modified cells should be reconsidered, although the possibility that these adverse events are HexA specific cannot be excluded. An example of overexpression-associated toxicity of a lysosomal enzyme in a particular target cell type is that described for *ex vivo* lentivirus gene therapy in Krabbe disease, where galactocerebrosidase proved to be toxic to hematopoietic stem cells but not to their progeny.[62] This has not been documented for other lysosomal enzymes where this *ex vivo* strategy has been successful for storage diseases such as metachromatic leukodystrophy.[63] Presently, the possibility that toxicity is the result of unique properties of cm hexosaminidase subunits cannot be excluded. Further studies with hexosaminidases from different species will be necessary to address this possibility.

The reasons for the difference in outcomes between NHPs and normal cats injected with AAVrh8 vectors carrying the same expression elements at comparable doses are unknown. It is possible the CBA promoter and/or WPRE in the transgene expression cassette have different potencies across species, and also that AAVrh8 transduces NHP cells more efficiently, given that it was cloned from rhesus macaque tissues.[64] The 3×10^{12} vg dose tested in NHP was based on a prior study[27] where GM2 cats were treated with 1.1×10^{12} vg of AAVrh8 vector delivered bilaterally to the thalamus and CSF via the lateral ventricle. The dose/brain weight is comparable at 5.3×10^{13} vg/kg, considering average brain weights of 60.4 ± 5.5 g and 20.9 ± 1.6 g in young cm and cats, respectively. An important aspect to consider is that the thalamic dose in cats was delivered in a columnar fashion, where the needle was raised 0.15 cm after each 10–20 μL bolus, while in NHP convection-enhanced delivery in a single site in the thalamus was used. The two infusion techniques likely generate different patterns of AAV vector distribution in the thalamus and possibly trans-

duction efficiency that might be reflected in differences in AAV genome copy number per cell. Nonetheless, a 30-fold reduction in AAV vector dose in NHP was insufficient to prevent toxicity in NHP. This suggests that differences in infusion technique and ultimately AAV distribution in thalamus are unlikely to explain the surprising difference in outcomes in monkeys and cats. The degree of neuronal loss documented in monkeys prevents a meaningful comparison of AAV vector genome content in the thalamus between the two species and others, as it is impossible to know how much of the initial dose has been lost in monkeys due to toxicity. Since dose reduction proved ineffective in preventing thalamic toxicity in monkeys, an alternative approach is to decrease transgene expression strength from the AAV vector. This may be accomplished through removal of the WPRE element and using weaker promoters. However, the optimization process will be mostly empirical because the available data on safe levels of hexosaminidase overexpression in the brain of other species injected with AAV-Hex[17,26,27] are at the tissue level comprised of AAV transduced and non-transduced cells. Presently, there is no information on the degree of enzyme overexpression in individual AAV transduced cells (neurons) in the brain that is compatible with long-term safety and efficacy. A recent study using systemic delivery of AAV9 encoding another lysosomal enzyme, α-N-acetylglucosaminidase, to treat mucopolysaccharidosis (MPS) IIIB resulted in liver toxicity associated with transgene overexpression in wild-type but not MPS IIIB mice.[65] The difference in safety outcomes across and within species raises concerns about the predictive value of preclinical dose ranging and safety studies when translating AAV gene therapies from animals to humans.

Prior studies assessing the safety of multisite intracranial delivery of AAVrh10 vectors in NHPs reported no serious adverse events.[46,66] However, neuropathological examination revealed cellular loss at the injection sites, but because the studies were carried out with AAVrh10 vectors encoding human enzymes, it is not possible to distinguish between an immunologically driven effect and toxicity due to overexpression as documented here. The absence of neurological side effects in those studies may simply be due to the small injection volumes per site (10 μL) in non-motor cortical regions where the effect of cellular loss in small numbers may not be easily detectable. The mechanistic basis for the cellular loss/spongiosis observed in those studies has different implications for the success in translation of these multisite approaches to patients. Clinical trials have been initiated with AAVrh10 vectors tested in NHPs and the outcomes in patients will ultimately reveal the safety and efficacy of the multisite delivery approach (NCT01801709).

Overexpression and secretion of lysosomal enzymes from genetically modified cells is the fundamental tenet of the current *ex vivo* and *in vivo* gene therapy approaches for lysosomal storage diseases. Though the exact tolerability limits for lysosomal enzyme overexpression in cells is unknown and may vary across enzymes, the notion that these proteins can be safely expressed at any level with no consequences should be evaluated carefully.

ACKNOWLEDGMENTS

We would like to thank Dr. Richard P. Moser, MD, for use of his MRI compatible stereotaxic frame. This work was supported by grants from Cure Tay–Sachs Foundation, National Tay–Sachs and Allied Diseases Association, and the National Institutes of Health (U01NS064096).

AUTHOR DISCLOSURE

No competing financial interests exist.

REFERENCES

1. Gravel RA, Kaback MM, Proia RL, et al. The GM2 gangliosidoses. In: Scriver C, Beaudet AL, Sly WS, Valle D, et al., eds. The Metabolic and Molecular Bases of Inherited Disease. New York: McGraw-Hill, 2001.
2. Bley AE, Giannikopoulos OA, Hayden D, et al. Natural history of infantile GM2 gangliosidosis. Pediatrics 2011;128:e1233–1241.
3. Desnick RJ, Schuchman EH. Enzyme replacement therapy for lysosomal diseases: lessons from 20 years of experience and remaining challenges. Annu Rev Genomics Hum Genet 2012;13:307–335.
4. Johnson WG, Desnick RJ, Long DM, et al. Intravenous injection of purified hexosaminidase A into a patient with Tay–Sachs disease. Birth Defects Orig Artic Ser 1973;9:120–124.
5. Enns GM, Huhn SL. Central nervous system therapy for lysosomal storage disorders. Neurosurg Focus 2008;24:E12.
6. Taylor RM, Wolfe JH. Decreased lysosomal storage in the adult MPS VII mouse brain in the vicinity of grafts of retroviral vector-corrected fibroblasts secreting high levels of beta-glucuronidase. Nat Med 1997;3:771–774.
7. Chang M, Cooper JD, Sleat DE, et al. Intraventricular enzyme replacement improves disease phenotypes in a mouse model of late infantile neuronal ceroid lipofuscinosis. Mol Ther 2008;16:649–656.
8. Liu G, Martins I, Wemmie JA, et al. Functional correction of CNS phenotypes in a lysosomal storage disease model using adeno-associated virus type 4 vectors. J Neurosci 2005;25:9321–9327.
9. Watson G, Bastacky J, Belichenko P, et al. Intrathecal administration of AAV vectors for the treatment of lysosomal storage in the brains of MPS I mice. Gene Ther 2006;13:917–925.

10. Broekman ML, Tierney LA, Benn C, et al. Mechanisms of distribution of mouse beta-galactosidase in the adult GM1-gangliosidosis brain. Gene Ther 2009;16:303–308.

11. Hennig AK, Levy B, Ogilvie JM, et al. Intravitreal gene therapy reduces lysosomal storage in specific areas of the CNS in mucopolysaccharidosis VII mice. J Neurosci 2003;23:3302–3307.

12. Hennig AK, Ogilvie JM, Ohlemiller KK, et al. AAV-mediated intravitreal gene therapy reduces lysosomal storage in the retinal pigmented epithelium and improves retinal function in adult MPS VII mice. Mol Ther 2004;10:106–116.

13. Luca T, Givogri MI, Perani L, et al. Axons mediate the distribution of arylsulfatase A within the mouse hippocampus upon gene delivery. Mol Ther 2005;12:669–679.

14. Passini MA, Lee EB, Heuer GG, et al. Distribution of a lysosomal enzyme in the adult brain by axonal transport and by cells of the rostral migratory stream. J Neurosci 2002;22:6437–6446.

15. Griffey M, Macauley SL, Ogilvie JM, et al. AAV2-mediated ocular gene therapy for infantile neuronal ceroid lipofuscinosis. Mol Ther 2005; 12:413–421.

16. Golebiowski D, Bradbury A, Kwon C-S, et al. AAV gene therapy strategies for lysosomal storage disorders with central nervous system involvement. In: Bo X, Verhaagen J, eds. Gene Delivery and Therapy for Neurological Disorders. New York: Springer, 2015:265–295.

17. Cachon-Gonzalez MB, Wang SZ, Lynch A, et al. Effective gene therapy in an authentic model of Tay–Sachs-related diseases. Proc Natl Acad Sci U S A 2006;103:10373–10378.

18. Bosch A, Perret E, Desmaris N, et al. Long-term and significant correction of brain lesions in adult mucopolysaccharidosis type VII mice using recombinant AAV vectors. Mol Ther 2000; 1:63–70.

19. Skorupa AF, Fisher KJ, Wilson JM, et al. Sustained production of beta-glucuronidase from localized sites after AAV vector gene transfer results in widespread distribution of enzyme and reversal of lysosomal storage lesions in a large volume of brain in mucopolysaccharidosis VII mice. Exp Neurol 1999;160:17–27.

20. Cearley CN, Wolfe JH. A single injection of an adeno-associated virus vector into nuclei with divergent connections results in widespread vector distribution in the brain and global correction of a neurogenetic disease. J Neurosci 2007;27:9928–9940.

21. Dodge JC, Clarke J, Song A, et al. Gene transfer of human acid sphingomyelinase corrects neuropathology and motor deficits in a mouse model of Niemann–Pick type A disease. Proc Natl Acad Sci U S A 2005;102:17822–17827.

22. Baek RC, Broekman ML, Leroy SG, et al. AAV-mediated gene delivery in adult GM1-gangliosidosis mice corrects lysosomal storage in CNS and improves survival. PloS One 2010;5:e13468.

23. Haurigot V, Marco S, Ribera A, et al. Whole body correction of mucopolysaccharidosis IIIA by intracerebrospinal fluid gene therapy. J Clin Invest 2013 Jul 1. DOI: 10.1172/JCI66778 [Epub ahead of print].

24. Liu G, Martins IH, Chiorini JA, et al. Adeno-associated virus type 4 (AAV4) targets ependyma and astrocytes in the subventricular zone and RMS. Gene Ther 2005;12:1503–1508.

25. Bradbury AM, Cochran JN, McCurdy VJ, et al. Therapeutic response in feline Sandhoff disease despite immunity to intracranial gene therapy. Molecular Ther 2013;21:1306–1315.

26. McCurdy VJ, Rockwell HE, Arthur JR, et al. Widespread correction of central nervous system disease after intracranial gene therapy in a feline model of Sandhoff disease. Gene Ther 2015;22: 181–189.

27. Rockwell HE, McCurdy VJ, Eaton SC, et al. AAV-mediated gene delivery in a feline model of Sandhoff disease corrects lysosomal storage in the central nervous system. ASN Neuro 2015;7.

28. Gurda BL, De Guilhem De Lataillade A, Bell P, et al. Evaluation of AAV-mediated gene therapy for central nervous system disease in canine mucopolysaccharidosis VII. Mol Ther 2016;24:206–216.

29. Hinderer C, Bell P, Gurda BL, et al. Intrathecal gene therapy corrects CNS pathology in a feline model of mucopolysaccharidosis I. Mol Ther 2014;22:2018–2027.

30. Katz ML, Tecedor L, Chen Y, et al. AAV gene transfer delays disease onset in a TPP1-deficient canine model of the late infantile form of Batten disease. Sci Transl Med 2015;7:313ra180.

31. Yoon SY, Bagel JH, O'Donnell PA, et al. Clinical improvement of alpha-mannosidosis cat following a single cisterna magna infusion of AAV1. Mol Ther 2016;24:26–33.

32. McCurdy VJ, Johnson AK, Gray-Edwards HL, et al. Sustained normalization of neurological disease after intracranial gene therapy in a feline model. Sci Transl Med 2014;6:231ra248.

33. Guidotti JE, Mignon A, Haase G, et al. Adenoviral gene therapy of the Tay–Sachs disease in hexosaminidase A-deficient knock-out mice. Hum Mol Genet 1999;8:831–838.

34. Arfi A, Bourgoin C, Basso L, et al. Bicistronic lentiviral vector corrects beta-hexosaminidase deficiency in transduced and cross-corrected human Sandhoff fibroblasts. Neurobiol Dis 2005;20:583–593.

35. Itakura T, Kuroki A, Ishibashi Y, et al. Inefficiency in GM2 ganglioside elimination by human lysosomal beta-hexosaminidase beta-subunit gene transfer to fibroblastic cell line derived from Sandhoff disease model mice. Biol Pharm Bull 2006;29:1564–1569.

36. Torres PA, Zeng BJ, Porter BF, et al. Tay–Sachs disease in Jacob sheep. Mol Genet Metab 2010; 101:357–363.

37. Cork LC, Munnell JF, Lorenz MD, et al. GM2 ganglioside lysosomal storage disease in cats with beta-hexosaminidase deficiency. Science 1977;196:1014–1017.

38. Martin DR, Krum BK, Varadarajan GS, et al. An inversion of 25 base pairs causes feline GM2 gangliosidosis variant. Exp Neurol 2004;187:30–37.

39. Cachon-Gonzalez MB, Wang SZ, McNair R, et al. Gene transfer corrects acute GM2 gangliosidosis—potential therapeutic contribution of perivascular enzyme flow. Mol Ther 2012;20:1489–1500.

40. Bevan AK, Duque S, Foust KD, et al. Systemic gene delivery in large species for targeting spinal cord, brain, and peripheral tissues for pediatric disorders. Mol Ther 2011;19:1971–1980.

41. Meyer K, Ferraiuolo L, Schmelzer L, et al. Improving single injection CSF delivery of AAV9-mediated gene therapy for SMA: a dose–response study in mice and nonhuman primates. Mol Ther 2015;23:477–487.

42. Murrey DA, Naughton BJ, Duncan FJ, et al. Feasibility and safety of systemic rAAV9-hNAGLU delivery for treating mucopolysaccharidosis IIIB: toxicology, biodistribution, and immunological assessments in primates. Hum Gene Ther Clin Dev 2014;25:72–84.

43. San Sebastian W, Kells AP, Bringas J, et al. Safety and tolerability of MRI-guided infusion of AAV2-hAADC into the mid-brain of non-human primate. Mol Ther Methods Clin Dev 2014;3.

44. Colle MA, Piguet F, Bertrand L, et al. Efficient intracerebral delivery of AAV5 vector encoding human ARSA in non-human primate. Hum Mol Genet 2010;19:147–158.

45. Cederfjall E, Nilsson N, Sahin G, et al. Continuous DOPA synthesis from a single AAV: dosing and efficacy in models of Parkinson's disease. Sci Rep 2013;3:2157.

46. Zerah M, Piguet F, Colle MA, et al. Intracerebral gene therapy using AAVrh.10-hARSA recombinant vector to treat patients with early-onset forms of metachromatic leukodystrophy: preclinical feasibility and safety assessments in nonhuman primates. Hum Gene Ther Clin Dev 2015;26:113–124.

47. Sondhi D, Peterson DA, Giannaris EL, et al. AAV2-mediated CLN2 gene transfer to rodent and non-human primate brain results in long-term TPP-I expression compatible with therapy for LINCL. Gene Ther 2005;12:1618–1632.

48. Broekman ML, Baek RC, Comer LA, et al. Complete correction of enzymatic deficiency and neurochemistry in the GM1-gangliosidosis mouse brain by neonatal adeno-associated virus-mediated gene delivery. Mol Ther 2007;15:30–37.

49. Zanta-Boussif MA, Charrier S, Brice-Ouzet A, et al. Validation of a mutated PRE sequence allowing high and sustained transgene expression while abrogating WHV-X protein synthesis: application to the gene therapy of WAS. Gene Ther 2009;16:605–619.

50. Broekman ML, Comer LA, Hyman BT, et al. Adeno-associated virus vectors serotyped with AAV8 capsid are more efficient than AAV-1 or -2 serotypes for widespread gene delivery to the neo-

natal mouse brain. Neuroscience 2006;138:501–510.

51. Calcedo R, Vandenberghe LH, Gao G, et al. Worldwide epidemiology of neutralizing antibodies to adeno-associated viruses. J Infect Dis 2009;199:381–390.
52. van der Bom IM, Moser RP, Gao G, et al. Finding the striatum in sheep: use of a multi-modal guided approach for convection enhanced delivery. J Huntingtons Dis 2013;2:41–45.
53. van der Bom IM, Moser RP, Gao G, et al. Frameless multimodal image guidance of localized convection-enhanced delivery of therapeutics in the brain. J Neurointerv Surg 2013;5:69–72.
54. Spetzler RF, Selman WR, Weinstein P, et al. Chronic reversible cerebral ischemia: evaluation of a new baboon model. Neurosurgery 1980;7:257–261.
55. Salegio EA, Samaranch L, Jenkins RW, et al. Safety study of adeno-associated virus serotype 2-mediated human acid sphingomyelinase expression in the nonhuman primate brain. Hum Gene Ther 2012;23:891–902.
56. Samaranch L, San Sebastian W, Kells AP, et al. AAV9-mediated expression of a non-self protein in nonhuman primate central nervous system triggers widespread neuroinflammation driven by antigen-presenting cell transduction. Mol Ther 2014;22:329–337.
57. Hadaczek P, Forsayeth J, Mirek H, et al. Transduction of nonhuman primate brain with adeno-associated virus serotype 1: vector trafficking and immune response. Hum Gene Ther 2009;20:225–237.
58. Bigger BW, Saif M, Linthorst GE. The role of antibodies in enzyme treatments and therapeutic strategies. Best Pract Res Clin Endocrinol Metab 2015;29:183–194.
59. van Gelder CM, Hoogeveen-Westerveld M, Kroos MA, et al. Enzyme therapy and immune response in relation to CRIM status: the Dutch experience in classic infantile Pompe disease. J Inherit Metab Dis 2015;38:305–314.
60. Vogler C, Galvin N, Levy B, et al. Transgene produces massive overexpression of human beta-glucuronidase in mice, lysosomal storage of enzyme, and strain-dependent tumors. Proc Natl Acad Sci U S A 2003;100:2669–2673.
61. Hiramatsu N, Chiang WC, Kurt TD, et al. Multiple mechanisms of unfolded protein response-induced cell death. Am J Pathol 2015;185:1800–1808.
62. Gentner B, Visigalli I, Hiramatsu H, et al. Identification of hematopoietic stem cell-specific miRNAs enables gene therapy of globoid cell leukodystrophy. Sci Transl Med 2010;2:58ra84.
63. Biffi A, Montini E, Lorioli L, et al. Lentiviral hematopoietic stem cell gene therapy benefits metachromatic leukodystrophy. Science 2013;341:1233158.
64. Gao G, Vandenberghe LH, Alvira MR, et al. Clades of adeno-associated viruses are widely disseminated in human tissues. J Virol 2004;78:6381–6388.
65. Meadows AS, Duncan FJ, Camboni M, et al. A GLP-compliant toxicology and biodistribution study: systemic delivery of an rAAV9 vector for the treatment of mucopolysaccharidosis IIIB. Hum Gene Ther Clin Dev 2015;26:228–242.
66. Sondhi D, Johnson L, Purpura K, et al. Long-term expression and safety of administration of AAVrh.10hCLN2 to the brain of rats and nonhuman primates for the treatment of late infantile neuronal ceroid lipofuscinosis. Hum Gene Ther Methods 2012;23:324–335.

Received for publication July 13, 2016;
accepted after revision January 23, 2017.

Published online: January 26, 2017.